Surface segregation at the binary alloy CuAu (100)

studied by Low-Energy Ion Scattering

Robert Beikler[1,2], Edmund Taglauer[1*]

[1]*Max-Planck-Institut für Plasmaphysik, D-85748 Garching bei München, Germany*

[2]*now at Munich Metrology, D-85551 Kirchheim bei München, Germany*

Abstract

We present results from an experimental study of segregation at the CuAu (100) surface. It is shown that Au enrichment in the top surface layer persists up to temperatures far beyond the bulk order-disorder transition temperature. From the gradual desegregation at higher temperatures a segregation energy of -0.30 eV was determined. Our results are in quantitative agreement with calculations by Tersoff predicting oscillatory concentration depth profiles with decreasing amplitudes at higher temperatures. For the layer selective surface analysis we used low-energy He^+ and Na^+ scattering. Data interpretation and quantification was supported by numerical simulations with the MARLOWE code to which we had added the special features of trajectory resolved analysis and anisotropic thermal vibrations of surface atoms.

1. Introduction

The surface composition of metallic alloys differs in many cases from that of the bulk. This phenomenon of surface segregation, i.e. the enrichment of one constituent in the surface region and at grain boundaries, is of fundamental interest and also of importance for technical areas such as metallurgy, catalysis, etc. A large number of experimental and theoretical investigations has therefore been dedicated to surface segregation [1-4]. Particularly binary alloys have been studied to reveal the underlying physical processes [4-6]. Strong pair interaction between the constituents often results in chemical ordering, i.e. each constituent occupies specific lattice sites in crystallographic order. For these cases the interplay between this chemical ordering and surface segregation is of special interest. Below the bulk order-disorder transition temperature, T_0, segregation means deviation from this ordering, above T_0 it means deviation from statistical site occupation. The segregation induced compositional depth profile reveals information about the binding characteristics of such alloys: monotonous profiles indicate weak pair interaction between the two constituents while oscillatory profiles result from stronger binding forces. It is therefore necessary to perform layer-selective

Corresponding author, e-mail: edmund.taglauer@ipp.mpg.de

composition analysis in the near-surface region. Here low-energy ion scattering (LEIS) can be applied with advantage, because it is extremely surface sensitive and provides compositional information exclusively for the top two or three surface layers [8-10].

The CuAu system studied in this work is a prototype of a weakly ordering metallic alloy with an order-disorder phase transition [1]. Generally it shows surface segregation of Au at elevated temperatures. Stable phases exist in the compositions Cu_3Au, $CuAu$, and $CuAu_3$. Most studies refer to the Cu_3Au phase [11], much less to $CuAu_3$ [12]. For CuAu only few experimental results are published in the literature [13-15]. Recent theoretical studies deal with density functional calculations of corresponding surface alloys [16] and with the structure of CuAu bimtetallic clusters [17]. A theoretical study by Tersoff [18] for CuAu (100) using an empirical potential for Monte Carlo calculations predicts Au segregation with an oscillating segregation depth profile, i.e. Au-rich layers alternate with Au depleted layers. The amplitudes of these oscillations decrease with increasing temperature.

In continuation of our previously reported work [13,14] we present here the temperature development of the surface segregation at CuAu (100) and compare our results with theoretical predictions. For this study we use He^+ and Na^+ ion scattering to analyze the composition of the first and second crystal layers as a function of temperature in the range below and above the bulk transition temperature T_0. For the quantitative interpretation of the experimental ion scattering data we make use of numerical simulations with the MARLOWE code [19] to which we had added extra features, in particular the possibility of trajectory resolved analysis [20].

2. Analytical method

Experiment

The experimental setup consists of an ultrahigh-vacuum chamber (base pressure 10^{-10}mbar) that is equipped with noble gas (He^+, Ne^+) and alkali (Li^+, Na^+) ion sources, a two-axis sample holder with heating and cooling facilities and an electrostatic energy analyzer, i.e. only scattered ions are detected and possible neutralization effects have to be kept in mind. The chamber also contains a 4-grid rear view LEED system for checking surface structures by electron diffraction.

Care has to be taken in preparing a clean and well ordered (100) surface of the CuAu crystal. The familiar cleaning procedure using Ar+ ion sputtering and heating below 200 °C does not show satisfactory results. CuAu(100) is known to have a 7% reduction of the lattice constant perpendicular to the surface, i.e. a tetragonal structure labeled the CuAuI phase [21]. Heating to higher temperatures therefore bares the danger of recrystallization. This can be overcome by rapid cooling with liquid nitrogen after heating above T_0 [22]. Applying this procedure we obtained clean and well ordered crystal surfaces.

Single crystalline alloy samples are required to enable unambiguous layer definition. Ion scattering is particularly sensitive for heavy elements as in our case here, but atomic position analysis is also possible for light elements such as hydrogen, in the recoil detection mode [23]. For layer selective scattering we have to choose the appropriate scattering geometry, i.e. for the (100) surface of a fcc crystal we take an angle of incidence relative to the surface of $\Psi = 45°$ and a scattering angle of $\Theta = 90°$. This way we observe almost exclusively first layer scattering along the [100] azimuth because lower lying atoms are shadowed, and scattering from layer 1 and 2 contributes for the [110] azimuth, see Fig. 1.
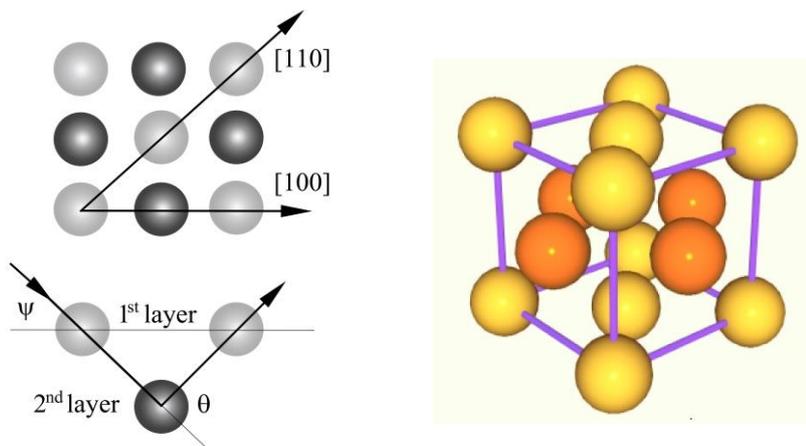

Fig. 1. Ball model of the CuAu unit cell, left side: upper panel top view, lower panel side view. Light balls show Au, dark balls Cu atoms. Selected scattering geometries are indicated by arrows, see text. Right side : 3D model.

Regarding the 7% relaxation mentioned above this scattering geometry is not quite optimal for CuAu(100), but we wanted to use the same scattering geometry as in the calibration measurements. The shadow cone caused by the top layer atoms still prevents scattering from second layer atoms in this geometry.

Calibration

For quantitative analysis the scattering yields have to be calibrated and this is best achieved by using elemental single crystals of the constituents of the alloy. For He[+] scattering from Au also good agreement between the ion yields from CuAu (100) and polycrystalline Au samples has been reported [24]. In our case we also use Cu (100) and Au (110) crystal surfaces for calibration. The structures of these surfaces are well known [8]: while Cu (100) has bulk termination, the low index Au surfaces are reconstructed, Au(110) exhibits a (1x2) surface structure at room temperature. The reconstructed surface can be identified in the azimuthal variations of the scattered ion intensities at grazing incidence [25], but this is not treated in the present context. He^{+} ion scattering provides information from the top atomic layer of the crystal due to neutralization of ions scattered from deeper layers. Since we are also interested in the composition of the second layer we additionally use Na^{+} ions that also give good mass resolution for Cu and Au. It is interesting to note that for He^{+} scattering from Cu and Au the difference in the cross sections is virtually exactly compensated by the higher neutralization for scattering from Au, such that the measured ion intensities can be taken for the relative atomic concentrations. A theoretical explanation of this effect is presently not given. For Na^{+} scattering the differences in the neutralization rates for Cu and Au are found to be very small and can be neglected. Corresponding results are shown below. Further discussions of the ion yields can be found in refs 24 and 12.

Simulation

The computer code MARLOWE [19] used here can be applied for three different sample structures, single crystal, polycrystal, and amorphous. The code is based on the binary collision approximation taking for the scattering potential a screened Coulomb potential,

$$V(r) = (Z_1 Z_2 e^2 / 4\pi\varepsilon_0 r)\Phi(r/a). \qquad (1)$$

The characteristic length a in the screening function Φ is determined by calibration measurements. It turns out that corrections to the frequently used Firsov screening length [26]

$$a_F = 0.4685/(\sqrt{Z_1} + \sqrt{Z_2})^2/3 \ (\text{Å}) \qquad (2)$$

have to be applied (Z_1 and Z_2 are the projectile and target nuclear charges, respectively). Thermal vibrations are treated according to the high temperature Debye approximation, the mean square vibration amplitudes $< \Delta u^2 >$ being given by

$$< \Delta u^2 > = 3\hbar^2 T/M^2 k \Theta_D^2 . \qquad (3)$$

M is the mass of the vibrating atom. The Debye temperature Θ_D is used as a calibration parameter to take thermal vibrations into account. Inelastic energy losses of the projectile to target electrons can be treated by using the local energy loss model (Oen-Robinson) or the continuous stopping concept dE/dx [19]. In the original MARLOWE code a combination of both is applied and was also used here. Neutralization processes are not included in the original MARLOWE version. For our purposes we therefore implemented extensions to the program that allow us to perform detailed trajectory analysis [25]. The data for each projectile trajectory are stored and specific sets can be produced according to various selection criteria. In this context we particularly consider the deepest crystal layer to which the projectile has penetrated. Furthermore a feature was implemented that allows to apply different thermal vibration parameters, i.e. to apply different Debye temperatures for surface and bulk atoms and to distinguish between vibrations parallel and perpendicular to the surface.

For Cu (100) the experimental energy distributions could be very well reproduced by adjusting the screening parameters and by applying adequate values for the surface Debye temperatures [20]. This was achieved by taking the non-isotropic values for vibrations perpendicular and parallel to the surface as calculated by Jackson [27].. A similar procedure was applied for the calibration with the Au(110)(1x2) surface. We thus obtained the following results from the calibrations:

Screening length for Na-Cu: 77% of a_F. Screening length for Na-Au: 95% of a_F. Such values are in agreement with other results reported in the literature [28].The Debye temperatures for Cu and Au calculated by Jackson from interatomic forces using Morse potentials [27] provide excellent agreement with our measured spectra. The fit of the simulation to one point (maximum in the Au peak) is sufficient to also reproduce the Cu intensity distribution without further fitting. We use these calibration parameters to study the surface composition and segregation on CuAu (100) in the temperature range below and above the bulk order-disorder transition temperature.

3. Results and discussion

The Cu and Au concentrations in the top layer are measured with He$^+$ ion scattering. The spectra in Fig.2 show the variation in surface composition with temperature. The Au concentration close to the transition temperature T_0 is about 95% and decreases with higher temperatures while the Cu concentration increases.
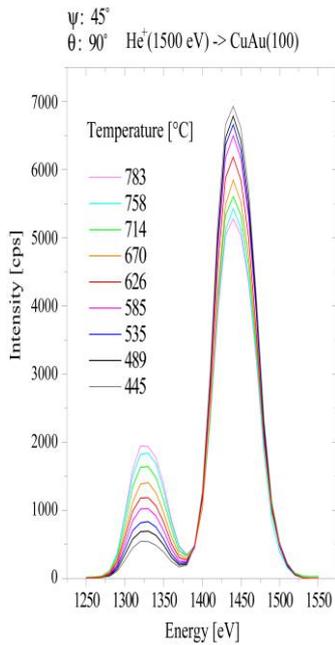

Fig. 2: Energy spectra for He$^+$ scattering from CuAu(100) at various crystal temperatures. Higher temperatures result in increasing Cu signals (1325 eV) and decreasing Au signals (1450 eV) from the top layer.

Information about first and second layer compositions are obtained from Na$^+$ scattering spectra. Fig. 3 shows experimental data and corresponding simulations (including the 7% inward relaxation in agreement with the tetragonal unit cell of CuAuI) [20]. The spectra taken in two different azimuthal directions show again that Au is the dominant species in the top layer whereas both, Cu and Au, are detected in layer 2. The experimental results are well reproduced by the simulations using our calibration parameters (without further fitting) and so quantitative evaluation is possible.
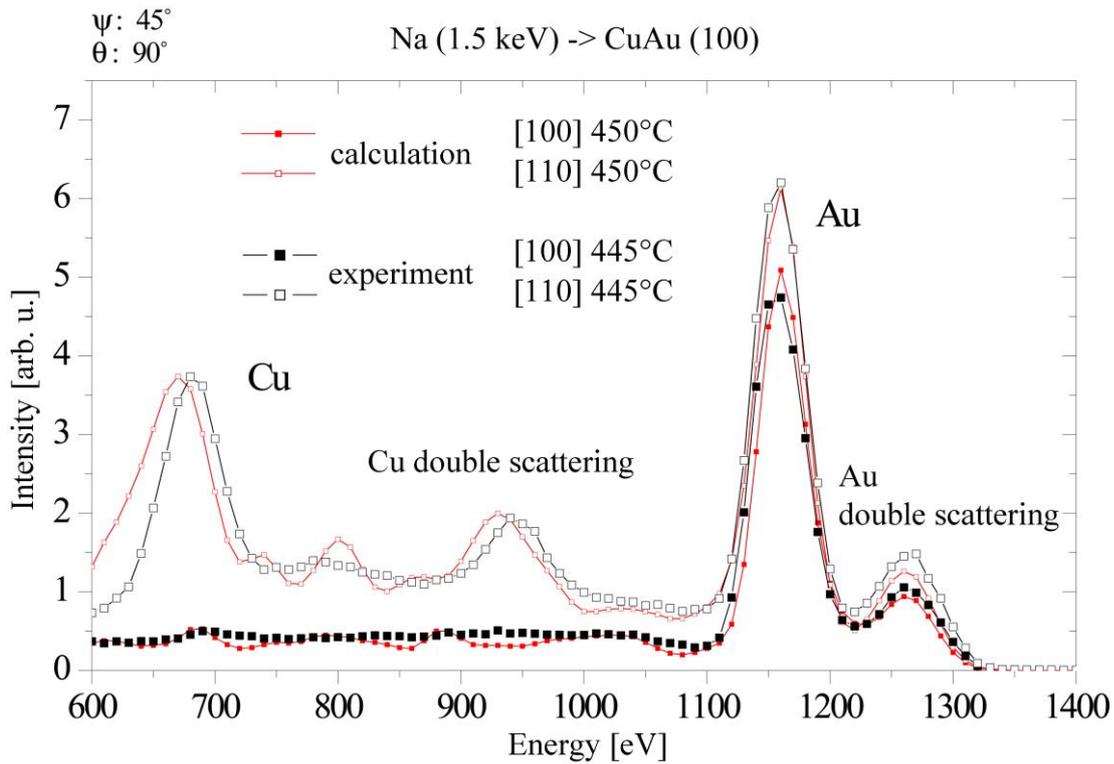
ψ: 45°
θ: 90°

Na (1.5 keV) -> CuAu (100)

Fig. 3: Experimental and calculated energy spectra for 1500 eV Na^+ scattering from CuAu (100) in two different azimuthal directions. Crystal temperature above T_0. Calculation for 95% Au in the first and 5% in the second layer [20].

The surface composition as a function of temperature range is obtained from quantitative evaluation of both, He^+ and Na^+ measurements. For this purpose the the Cu and Au concentrations in the surface layers were varied in the simulations until the best agreement between measured and calculated spectra was obtained. Figure 4 shows the results for the temperature range between -100 °C and 850 °C. For these measurements the crystal was heated up to the relevant temperature of each data point. At temperatures below T_0 rapid cooling with liquid nitrogen was necessary for reasons given in the experimental section. At temperatures around 0° C and below bombardment induced damage causes mixing in the surface layers.
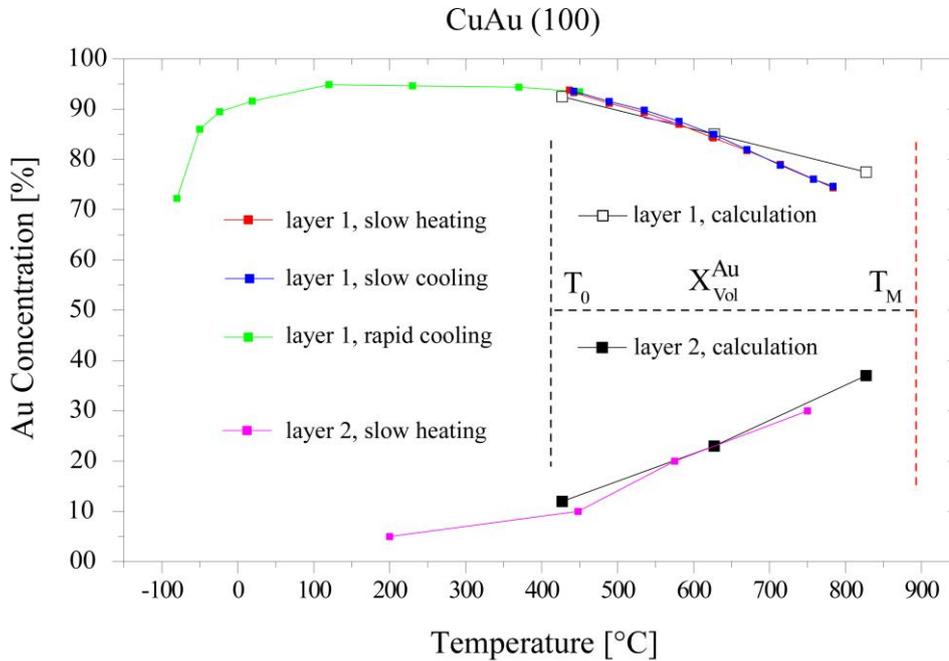
CuAu (100)

Fig. 4: Temperature dependence of the first and second layer Au concentrations on CuAu (100). T_0 is the bulk order-disorder transition temperature, T_M the melting point. The horizontal dashed line indicates the volume concentration at statistical mixing. Calculated data are taken from Tersoff [18].

For the top layer we find a Au concentration of about 95% in the lower temperature region, and only about 5% in the second layer. These two layers so represent a layering parallel to the (100) plane according to a $L1_0$ structure. The remaining small Au concentration in the second layer indicates a slight deviation from ideal bulk termination.

For temperatures above about 400°C entropic desegregation is observed. But the results clearly show that Au segregation persists up to temperatures close to the melting point T_M. The value of 50% for the high temperature bulk phase, indicated by the horizontal dashed line, is by far not obtained. In order to minimize the surface energy Au segregation obviously dominates over temperature induced entropic mixing. The gradual concentration change in both layers is in contrast to the discontinuous extinction of the ordering at $T_0 = 410$°C in the bulk phase. Our results thus indicate a continuous phase transition in the surface region. The asymmetric development of the Au concentrations in the two layers relative to the bulk value X^{Au}_{Vol} is also a sign of a damped oscillating concentration depth profile, similar to the case of Cu_3Au [5,11].

Fig. 4 also contains the data from the Monte Carlo calculations by Tersoff [16] , showing very good agreement with our results. Note that here we compare absolute values without any fitting. Our results thus confirm these theoretical predictions and the explanation that the surface energy difference drives Au to the surface layer and bonds between unlike atoms lead to Cu enrichment in the second layer. This way an oscillatory concentration profile develops which, according to Tersoff, decays exponentially into the bulk above the bulk ordering transition temperature T_0.

At higher temperatures gradual desegregation is observed, i.e. decrease of the Au concentration in the first layer accompanied by increasing Au concentration in the second layer. The degree of desegregation can be used to estimate the segregation energy ΔH. A Langmuir-McLean relation has been frequently applied [2] to describe temperature dependence of the concentration X of the segregating species with segregation energy ΔH according to

$$\frac{X^{surface}}{1 - X^{surface}} = \frac{X^{bulk}}{1 - X^{bulk}} \cdot e^{-\frac{\Delta H}{kT}} \qquad (4)$$

The corresponding evaluation of the Au concentration in layer 1 is shown in Fig. 5 and yields a segregation energy of $\Delta H = -0.30$ eV. This is less than the value of -0.5 eV reported by Schömann et al. [12] for $CuAu_3$, this value being in agreement with calculations for dilute solutions by Nørskov et al. [29]. They also predict a tendency to more positive values for increasing Au concentrations. This would support the relation of our result for ΔH compared to $CuAu_3$ under the assumption that the calculation for dilute solutions is applicable for our case.
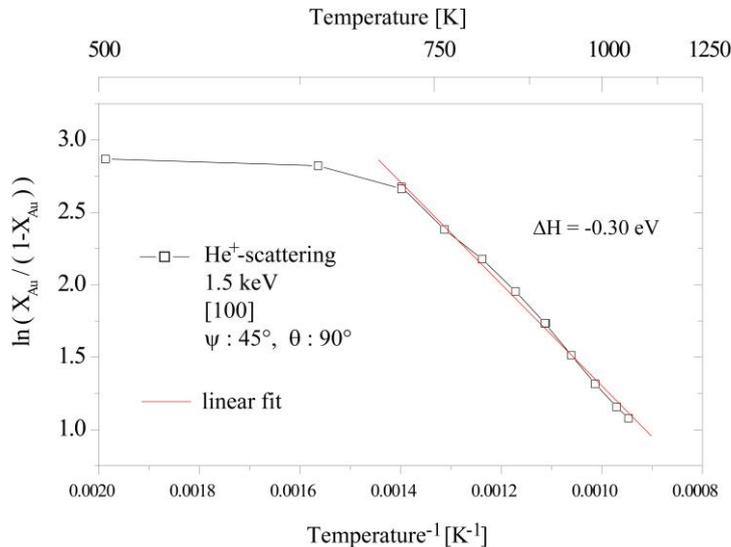
Fig. 5: Arrheniusplot of the first layer Au concentration on CuAu (100) for the determination of the segregation energy ΔH.

4. Summary

Detailed investigation of surface segregation requires layer resolved composition analysis as a function of temperature. It is shown that low-energy ion scattering can convey such information beyond first layer chemical composition. For quantitative evaluation of multiple scattering contributions numerical simulations with computer codes such as the MARLOWE code used in this work are necessary. We additionally developed trajectory resolved analysis that eases calibration, allows for identification of focusing effects, determination of potential parameters, inclusion of (non-isotropic) vibrational amplitudes, application of neutralization models and layer dependent composition analysis.

We used these methods to investigate the surface segregation at the binary alloy surface CuAu (100). Our experimental results show 95% Au concentration in the first layer and 5% in the second layer below the bulk order-disorder transition temperature T_0. Above T_0 gradual desegregation with increasing temperatures is observed, segregation persisting up to temperatures close to the melting point. We thus observe a continuous phase transition in the surface region. These results are in quantitative agreement with the calculations of Tersoff which give an oscillatory composition depth profile with gradually decreasing amplitudes at higher temperatures. From the decrease of the first layer Au concentration with temperature a segregation energy of -0.30 eV was determined.

References

[1]   P.A. Dowben, A. Miller, Eds.: *Surface Segregation Phenomena*, CRC Press, Boca Raton (1990).

[2]   J. du Plessis, *Surface Segregation*, Series Solid State Phenomena Vol. 11, Sci. Tech. Publ., Vaduz (1990).

[3]   U. Bardi, Rep. Progr. Phys 57 (1994) 939.

[4]   *Surface Alloys and Alloy Surfaces,* D, Woodruff Ed., Elsevier 2002

[5]   M. Polak and R. Rabinovich. Surf. Sci. Rep. 38 (2000) 127.

[6]   M. Schmid and P. Varga in: *The Chemical Physics of Solid Surfaces*, Vol. 10, Ed. D.P. Woodruff, Elsevier (2002) 118.

[7]   M.A. Vasiliev, J. Phys. D: Appl. Phys. 30 (1997) 3037

[8]   H. Niehus, W. Heiland, E. Taglauer Surf. Sci. Rep. 17 (1993) 213.

[9]   E. Taglauer in: *Surface Analysis*, Ed. J. Vickerman, Wiley, New York (1997) 215.

[10]   H.H. Brongersma, M. Draxler, M. de Ridder, P. Bauer, Surf. Sci. Rep. 62 (2007) 63.

[11]   T.M. Buck, G.H. Wheatley, L. Marchut, Phys. Rev. Lett. 64 (1990) 2527.

[12]   S. Schömann and E. Taglauer, Surf. Rev. Lett. 3 (1996) 1823.

[13]   R. Beikler and E. Taglauer, Nucl, Instr. Meth. Phys. Res. B161-163 (2000) 390.

[14]   E. Taglauer, R. Beikler, Vacuum 73 (2004) 9.

[15]   W. Schweika, H. Reichert, W. Babik, O. Klein. S. Engemann, Phys. Rev. B 70 (2004) 041401

[16]   M. J. Harrison, D.P. Woodruff, J. Robinson, Surf. Sci. 572 (2004) 309.

[17]   D. Cheng, S. Huang, W. Wang, Europ. Phys. J. D 39 (2006) 41.

[18]   J. Tersoff, Phys. Rev. B 42 (1990) 10965

[19]   M.T. Robinson and I.M. Torrens, Phys. Rev. B 9 (1974) 5008.

[20]   R. Beikler and E. Taglauer, Nucl. Instr. Meth. Phys. Res. B193 (2002) 455.

[21]   C. H. Johannson, J.O, Linde, Ann. Phys. 25 (1935) 1.

[22]   H. Reichert, private communication

[23]   J. Schulz, E. Taglauer, P. Feulner, D. Menzel, Nucl. Instr. Meth. Phys. Res. B64 (1992) 588.

[24]   D. Primetzhofer, M. Spitz, S. N. Markin, E. Taglauer, P. Bauer, Phys. Rev. B 80 (2009) 125425.

[25]   R. Beikler, E. Taglauer, Nucl. Instr. Meth. Phys. Res. B 182 (2001) 180.

[26]   O. Firsov, Sov. Phys. JETP 33 (1957) 696.

[27]   D.P. Jackson, Surf. Sci. 43 (1974) 431.

[28]   D. Primetzhofer, S. N. Markin, M. Draxler, R. Beikler, E. Taglauer, P. Bauer, Surf. Sci. 602 (2008) 2921.

[29]   J. K. Nørskov, B. Lundquist, Phys. Rev. 19 (1979) 5661.